RP Materials: Proceedings
Vol. 2, Part 1 (2023) pp. 29–35
e-ISSN: 2583-8342

RESEARCH PLATEAU PUBLISHERS

Cite this article: D. Singh, Operating features of parametric amplification in magnetoactive $A^{III}B^{V}$ semiconductor crystals, *RP Materials: Proceedings* Vol. 2, Part 1 (2023) pp. 29–35.

Original Research Article

Operating features of parametric amplification in magnetoactive $A^{III}B^{V}$ semiconductor crystals

Devender Singh*
Department of Physics, Government College, Matanhail, Jhajjar – 124106, Haryana, India
*Corresponding author, E-mail: dsdudi79@gmail.com

****Selection and Peer-Review under responsibility of the Scientific Committee of the International Conference on Recent Trends in Materials Science & Devices 2023 (ICRTMD 2023).**

ARTICLE HISTORY
Received: 10 May 2023
Revised: 20 Aug. 2023
Accepted: 22 Aug. 2023
Published online: 11 Sept. 2023

KEYWORDS
Parametric gain; piezoelectricity; magnetostatic field; $A^{III}B^{V}$ semiconductor.

ABSTRACT
Using a hydrodynamic model of semiconductors, it has been determined how doping concentrations and a transverse external magnetostatic field affect the operating features of parametric amplification of backward Stokes signals in the far infrared zone. Three attainable resonance situations are proposed by the model: These conditions have been used, on the one hand, to significantly lower the value of threshold intensity for onset of the parametric amplification and, on the other hand, for switching of parametric large positive and negative gain coefficient (i.e. amplification and absorption). These conditions include (i) lattice frequency and plasma frequency; (ii) Stokes frequency and electron-cyclotron frequency; and (iii) Stokes frequency and hybrid (plasma and electron-cyclotron) frequency. For instance, a strong 10.0 T transverse magnetostatic field with a 1.5×10^{19} m^{-3} free carrier concentration increases gain by a factor of 10^3 compared to when it is absent. The findings also point to a possible host for a parametric amplifier/frequency converter: a weakly piezoelectric $A^{III}B^{V}$ semiconductor that has been properly illuminated by slightly off-resonant, not-too-high power pulsed lasers with pulse duration sufficiently bigger than the acoustic phonon lifespan.

1. Introduction

Due to the variety of potential applications, the study of parametric interactions and the instruments that support them, such as optical parametric amplifiers and oscillators (OPA/OPO), have a unique position in nonlinear optics. It is widely utilised to create tunable coherent radiation sources with high gain and high conversion efficiency using optical parametric amplifiers and oscillators [1]. Successful applications of parametric interactions include the research of photon amplifiers [2, 3] and the production of high peak power subpicosecond optical pulses [4]. Designing and creating parametric amplifiers and oscillators requires careful consideration of the nonlinear medium to be used as well as the operating wavelength. Amongst different types of nonlinear media, semiconductors offer considerable flexibility for fabrication of optoelectronic devices because: (i) the large number of free electrons/holes available as majority charge carriers in doped semiconductors manifests many more exciting nonlinear optical processes [5]; (ii) carrier relaxation times can be altered through design of materials and device structures; (iii) large optical nonlinearities in the vicinity of band gap resonant transitions [6, 7]; (iv) either change in absorption or refractive index can be utilized; (v) devices may operate either at normal incidence or in waveguides; (vi) devices are integrable with other optoelectronic components, (vii) substantially transparent for photon energies less than the band gap energies [8]. It is important to note that semiconductors' optical nonlinearity, both resonant and non-resonant, has been used to create nonlinear optical devices. Resonant nonlinearities have a big magnitude [9], whereas SNON has a modest magnitude but a fast response time because of virtual transition mechanisms. Different kinds of nonlinear materials have been employed in the design and development of effective parametric amplifiers and oscillators [10, 11]. The increasing expansion of planar add-drop filters in advanced networks, however, shows that there is still a strong need to investigate alternatives, particularly ones compatible with semiconductor technology. Using bidirectional data injection and an additional external continuous wave signal for differentially biassing the interferometer arms, a hybridly integrated semiconductor optical amplifier Mach-Zehnder interferometer (MZI) was demonstrated, maximising gain and phase conditions during the switching functionality [12]. A long period linear grating is imprinted on a semiconductor waveguide, and its high frequency frequency converters are experimentally proved using second-order susceptibility [13].

It is common knowledge that controlling the threshold condition and gain is crucial to enhancing the effectiveness and usefulness of parametric devices (such as amplifiers, oscillators, and frequency converters). Doping (free carriers), composition, and micro-structuring have been primarily utilised in the case of semiconductors to enhance the performance of optoelectronic devices [14, 15]. Additionally, the ability of semiconductors' optical nonlinearities to be readily altered by externally applied electric and magnetic fields has been used to understand the mechanisms underlying

nonlinear processes like electro-optic and magneto-optic effects and to create devices based on them [16, 17]. Acoustic waves can generate optical second harmonic generation (SHG) in single and polycrystalline InAs, and Makowska et al. [18] discovered that the effectiveness of SHG relies on acoustic intensity. The efficiency of nonlinear interaction is significantly increased at the nonlinear resonances, nevertheless, in the case of the layered periodic structure of the $A^{III}B^{V}$ semiconductor-plasma [19]. Terahertz emission and photo-refraction in $A^{III}B^{V}$ semiconductors have been improved using the Voigt geometrical configuration [16, 17]. The second order susceptibility of weakly piezoelectric n-type $A^{III}B^{V}$ semiconductors has recently been the subject of comprehensive investigation [20] into the effects of free carrier concentration, an external magnetostatic field, and excitation intensity. The model [20] has been further expanded in the current article to evaluate parametric amplification operational characteristics and investigate the potential for switching optical nonlinearity by applied magnetostatic field. Expressions for operational characteristic parameters of parametric amplifiers, such as threshold condition and parametric gain, have been developed using the coupled-mode theory. Finally, exhaustive numerical analysis is performed with a set of data appropriate for weakly piezoelectric semiconductor-plasma (*n*-InSb) duly irradiated by a 10.6 μm CO_2 laser to establish the application of the present model. The findings show that changing the doping concentration, magnetostatic field, and excitation intensity can change the threshold condition and parametric gain.

2. Theoretical formulations

In the following section, it is shown how weakly piezoelectrically doped $A^{III}B^{V}$ semiconductors can be used to express the threshold condition for the onset of the backward coherent scattered stokes wave and its gain coefficient in both the absence and presence of an externally applied magnetostatic field.

In doing so we assume the pump wave (laser) energy ($\hbar\omega_p$) < band gap energy ($\hbar\omega_g$) of semiconductor. Since the laser pulse duration is significantly longer than the material damping time, the interaction is considered to be of the steady-state variety. We also take into account the fact that the pump wave is a plane wave and contains a lot of photons. The three-wave mixing mechanism within matter in the presence of an external magnetostatic field is described. The three waves are the pump wave, the backward scattered stokes wave, and the acoustic signal wave. We assume the pump electric field $E_p(x,t) = E_0 \exp[i(k_p x - \omega_p t)]$ is polarised along z-axis and incident on (110) surface of the crystal. Let us assume the electric field of pump radiation produces longitudinal acoustic wave (*i.e.* idler wave), $u(x,t) = u_0 \exp[i(k_a x - \omega_a t)]$ and in turn it scatters the pump wave. We further assume that the backward scattered stokes wave, say $E_s(x,t) = E_s \exp[i(k_s x - \omega_s t)]$, is also polarised along z-axis. In order to study parametric amplification in Voigt geometry an external transverse magnetostatic field (B_0) is applied parallel to z-axis.

The momentum and energy transfer between these waves can be described by phase matching conditions: $\hbar\vec{k}_p = \hbar\vec{k}_s + \hbar\vec{k}_a$ and $\hbar\omega_p = \hbar\omega_s + \hbar\omega_a$, where the frequencies $\{\omega_p, \omega_s, \omega_a\}$ and wave vectors $\{k_p, k_s, k_a\}$ correspond to the incident laser, the backward scattered Stokes wave and the acoustic wave, respectively. We also consider hydrodynamic model of the homogeneous one component (viz., *n*-type) semiconductor, satisfying the condition $k_a l << 1$ (k_a and l being the acoustic wave number and the electron mean free path, respectively). According to this circumstance, the mean free path of electrons is significantly longer than the sound wavelength, averaging out the mobility of the carriers under the effect of the external field. Additionally, it permits disregarding the dipole-approximated high frequency electric field's non-uniformity [21].

The zeroth-order electron momentum transfer equation under the influence of magnetostatic field can be described as:

$$\frac{\partial \vec{v}_0}{\partial t} + \gamma \vec{v}_0 = -e_1[\vec{E}_p + (\vec{v}_0 \times \vec{B}_0)] \tag{1}$$

where $e_1 = e/m$.

The first-order electron momentum transfer and continuity equation in the presence of external magnetostatic field are defined [20] by

$$\frac{\partial \vec{v}_1}{\partial t} + \gamma \vec{v}_1 + \vec{v}_0 \times (\nabla . \vec{v}_1) = -e_1[\vec{E}_1 + (\vec{v}_1 \times \vec{B}_0)] \tag{2}$$

$$\frac{\partial n_1}{\partial t} + n_0 \frac{\partial \vec{v}_1}{\partial x} + n_1 \frac{\partial \vec{v}_0}{\partial x} + \vec{v}_0 \frac{\partial n_1}{\partial x} = 0 \tag{3}$$

where $\vec{v}_0$ and $\vec{v}_1$ are zeroth- and first-order oscillatory fluid velocities of the electron of effective mass *m* and charge *–e*. n_0 and n_1 are initial and perturbed electron density and γ is the electron collision frequency. It is a well-known fact that the effective mass of an electron in III–V semiconductors is smaller than the effective mass of a hole and therefore the drift velocity of a hole is less than the drift velocity of an electron and hence the effect of hole on nonlinearity can be neglected.

The pump wave produces stress in the medium and the linear relationship between stress and electric field is described by piezoelectricity. The origin of piezoelectricity lies in the first order force ($f_1 = \beta(\partial E/\partial x)$, where β is piezoelectric coefficient). In particular, in narrow bandgap weakly piezoelectric $A^{III}B^{V}$ semiconductors such as InSb and InAs, the high mobility of electrons (due to their low effective mass) allows one to work at drift velocities several times the sound velocity and keep effects of inhomogeneities to minimum [22].

Let us consider, if the deviation of lattice along x-direction is $u(x, t)$, due to stress in the medium, in the presence of an external magnetostatic field then the strain can be described as $\partial u/\partial x$ and the resultant polarisation (P_{in}) can be given as:

$$P_{in} = \pm\beta(\partial u/\partial x) \tag{4}$$

Taking into account effect of piezoelectricity, the modified equation of motion of lattice vibrations may be defined as:

$$\frac{\partial^2 u}{\partial t^2} - \frac{C}{\rho}\frac{\partial^2 u}{\partial x^2} + 2\zeta_a \frac{\partial u}{\partial t} - \frac{\beta}{\rho}\frac{\partial E_1}{\partial x} = 0 . \tag{5}$$

where ρ, C and ζ_a being the mass density, material's elastic constant, acoustic phonon damping parameter and E_1 is being space charge electric field of the medium given as:

$$\frac{\partial E_1}{\partial x} = -\frac{n_1 e}{\varepsilon} - \frac{1}{C}\frac{\partial P_{in}}{\partial x}. \tag{6}$$

The expression for the piezoelectric doped semiconductors' first order perturbed carrier density caused by three-wave mixing is now of interest to us. Equations (1) through (6) are used to obtain a simpler equation for the density perturbation under the rotating wave approximation.

$$\frac{\partial^2 n_1}{\partial t^2} + \gamma_{eff}\frac{\partial n_1}{\partial t} + \Omega_p^2 n_1 A_1 \mp \frac{i\beta^2 k_a^3 \Omega_p^2 A_1 E_a}{\rho e \Delta_a^2} \pm \frac{ik_p \Omega_p^2 E_p n_1 e_1}{\Delta_{pl}^2} \mp \frac{\beta^2 k_p \Omega_p^2 E_p k_a^3 E_a}{\rho m \Delta_a^2 \Delta_{pl}^2} - e_1 A_0 E_p \frac{\partial n_1}{\partial x} - ie_1 n_1 A_0 k_p E_p = 0 \tag{7}$$

where $\Omega_p = (n_0 e^2/m\varepsilon)^{1/2}$ (electron-plasma frequency),

$\omega_c = e_1 B_0$ (electron-cyclotron frequency),

$\delta_p = \gamma - i\omega_p$, $\delta_1 = \gamma - i\omega_s + ik_s v_0$,

$A_0 = 1 - \frac{\omega_c^2}{\delta_p^2 + \omega_c^2}$, $A_1 = 1 - \frac{\omega_c^2}{\delta_1^2 + \omega_c^2}$,

$\gamma_{eff} = \gamma + ik_p v_0$, $\Delta_a^2 = -\omega_a^2 + k_a^2 v_a^2 - 2i\zeta_a \omega_a$,

and $\Delta_{pl}^2 = \frac{(\delta_p^2 + \omega_c^2)(\delta_1^2 + \omega_c^2)}{\delta_p \delta_1}$.

In obtaining Equation (7) we have neglected the Doppler shift under the assumption that $\omega_p >> k_a v_a$ (v_a being the velocity of an acoustic wave) and higher order terms like $n_0 v_0 (\partial^2 v_1 / \partial x \partial t)$. Equation (7) states that density perturbation may oscillates at low (acoustic, ω_a) and high (stokes, ω_s) wave frequency components and that can be expressed as: $n_1 = n_{1s}(\omega_a) + n_{1f}(\omega_s)$. The higher-order terms with frequencies $\omega_{s,q} (= \omega_p \pm q\omega_a)$, for $q \geq 2$ will be off-resonant and are neglected in the study of second-order nonlinearities in doped semiconductors. Using phase matching conditions, low and high frequency density perturbation can be obtained from Equation (7) as:

$$\frac{\partial^2 n_{1s}}{\partial t^2} + \gamma_{eff}\frac{\partial n_{1s}}{\partial t} + \Omega_p^2 n_{1s} A_1 \mp \frac{i\beta^2 k_a^3 \Omega_p^2 A_1 E_a}{\rho e \Delta_a^2} - ie_1 A_0 k_a n_{1f}^* E_p = 0 \tag{8}$$

and

$$\frac{\partial^2 n_{1f}}{\partial t^2} + \gamma_{eff}\frac{\partial n_{1f}}{\partial t} + \Omega_p^2 n_{1f} A_1 + ie_1 k_p \Omega_p^2 \Delta_{pl}^2 E_p n_{1s}^* \mp \frac{\beta^2 k_p \Omega_p^2 E_p k_a^3 E_a^*}{\rho m \Delta_a^2 \Delta_{pl}^2} - ie_1 A_0 k_s n_{1s}^* E_p = 0. \tag{9}$$

By solving coupled Equations (8) and (9), expression of n_{1s} (low frequency component) and n_{1f} (high frequency component) can be obtained as well as their values may be computed by using material parameters and electric field amplitudes in the absence and presence of transversely applied magnetostatic field. The expression of n_{1s} is obtained as:

$$n_{1s}^* = -\frac{i\beta^2 \Omega_p^2 k_a^3 E_a^*}{\rho \Omega_{pl}^2}\left[\pm\frac{A_1^*}{e\Delta_a^{2*}} \mp \frac{eA_0^* k_p k_a |E_p|^2}{m^2 \Delta_a^2 \Omega_{pd}^2 \Delta_{pl}^2}\right], \tag{10}$$

where

$$\Omega_{pl}^2 = \Omega_p^2 A_1 - \omega_a^2 = -i\gamma_{eff}\omega_a \text{ and } \Omega_{pd}^2 = \Omega_p^2 A_1 - \omega_s^2 = -i\gamma_{eff}\omega_s.$$

By knowledge of the first-order carrier density perturbation, second-order polarisation at backward Stoke's frequency can be obtained by time integral of induced current density ($J^{(2)}(\omega_s) = -n_{1s}^* e v_0$) as:

$$P^{(2)}(\omega_s) = \varepsilon_0 \chi^{(2)} E^2 = \int J^{(2)}(\omega_s) dt. \tag{11}$$

Using Equations (10) and (11), effective second-order optical complex susceptibility is obtained as:

$$\chi_{eff}^{(2)}(\omega_s) = \pm(\chi^{(2)}(\omega_s))_\beta \mp (\chi^{(2)}(\omega_s))_{\beta,I}, \tag{12}$$

where

$$(\chi^{(2)}(\omega_s))_\beta = \frac{i\beta^2 \Omega_p^2 k_a^3 A_1^* e_1 \delta_p}{\varepsilon_0 \rho \Delta_a^{2*} \Omega_{pl}^2 (\delta_p^2 + \omega_c^2)} \tag{12a}$$

$$(\chi^{(2)}(\omega_s))_{\beta,I} = \frac{2i\beta^2 \Omega_p^2 k_a^4 e_1^3 A_p^* k_p \delta_p I_p}{\varepsilon_0^2 \eta c \rho \Delta_a^2 \Omega_{pd}^2 \Omega_{pl}^2 \Delta_{pl}^2 (\delta_p^2 + \omega_c^2)} \tag{12b}$$

with $I_p = \frac{1}{2}\eta\varepsilon_0 c |E_p|^2$.

The real and imaginary parts of Equations (12a) and (12b) can be expressed using algebra. It is common knowledge that the real and imaginary components of optical susceptibility, respectively, represent crystallographic phenomena like refraction and gain/absorption. Numerous optical devices, including optical wave guides, filters, amplifiers, oscillators, and couplers, have been designed and manufactured using knowledge of the propagation of light in refractive media [11, 17]. The present article is focused to study behavior of the threshold condition for parametric amplification and gain

coefficient ($g(\omega_s)$) of backward coherent scattered stoke mode by varying free carrier density and externally applied magnetostatic field. In doing so, well known following expression [1] is used

$$g(\omega_s) = \frac{\omega_s}{\eta c}\left[(\chi^{(2)}(\omega_s))_{imag}\right]\left|E_p\right|. \quad (13)$$

3. Results and discussion

In order to explore the applicability of the model, a detailed numerical study of threshold condition and gain behavior of parametric amplification has been made. Efforts are also made to find out conditions for achieving large gain with low power laser. In doing so, we consider the irradiation of *n*-type doped $A^{III}B^{V}$ micro size semiconductor sample (such as InSb) by 10.6 μm CO_2 laser at liquid nitrogen temperature (77 K). Around this temperature, absorption coefficient of the sample is low around 10 μm and one may neglect contribution due to band to-band transition mechanism. It is worth pointing that at 77 K temperature, the dominant mechanism for transfer of momentum and energy of the electron in scattered mode is due to the acoustic phonon scattering in semiconductors [23, 24].

The following material parameters are taken as representative values to establish the theoretical formulation:

$\omega_p = 1.78\times10^{14}$ s^{-1}, $\omega_a = 2\times10^{11}$ s^{-1}, $\omega_s = 1.77\times10^{14}$ s^{-1},
$m = 0.014m_0$ (m_0 being the rest mass of an electron),
$\varepsilon_l = 15.8$, $\rho = 5.8\times10^3$ kg m^{-3}, $\eta = 3.8$, $\beta = 0.054$ cm^{-2},
$\gamma = 3\times10^{11}$ s^{-1}, $v_a = 4\times10^3$ ms^{-1}, $k_a = 5\times10^7$ m^{-1}.

The threshold pump intensity (I_{pth}) required for the onset of parametric amplification is obtained by setting imaginary part of Equation (12) equals to zero. I_{pth}, obtained from Equation (12a), versus with an external magnetostatic field for two different free carrier concentrations *i.e.* (a) $n_0 = 1.5\times10^{19}$ m^{-3} and (b) $n_0 = 2.4\times10^{19}$ m^{-3} is plotted in Figure 1. One may notice that in the absence of magnetostatic field, a large I_{pth} is required for onset of parametric amplification. For example, when $B_0 = 0.0$ T, we found $I_{pth} \sim 3.7\times10^8$ Wm^{-2} and 3.0×10^6 Wm^{-2} for $n_0 = 1.5\times10^{19}$ m^{-3} and 2.4×10^{19} m^{-3}, respectively.

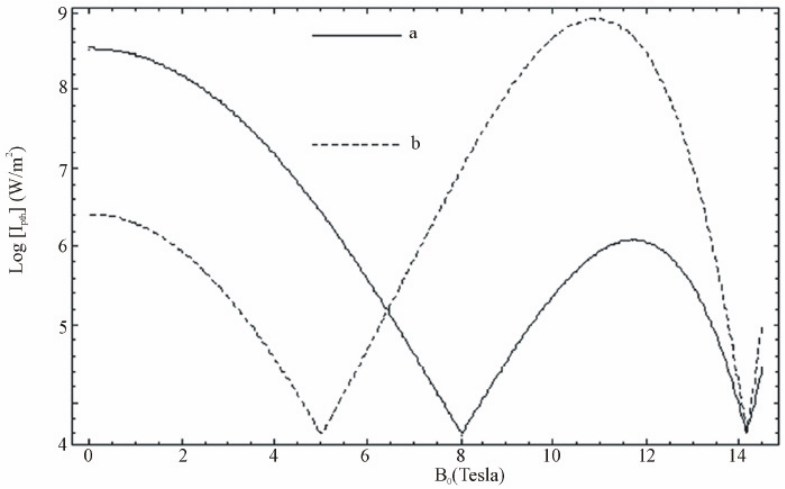

Figure 1: Variation of threshold pump intensity (Log [I_{pth}]), for Equation (12a), with magnetostatic field (B_0) at free carrier concentration (a) $n_0 = 1.5\times10^{19}$ m^{-3} and (b) $n_0 = 2.4\times10^{19}$ m^{-3}.

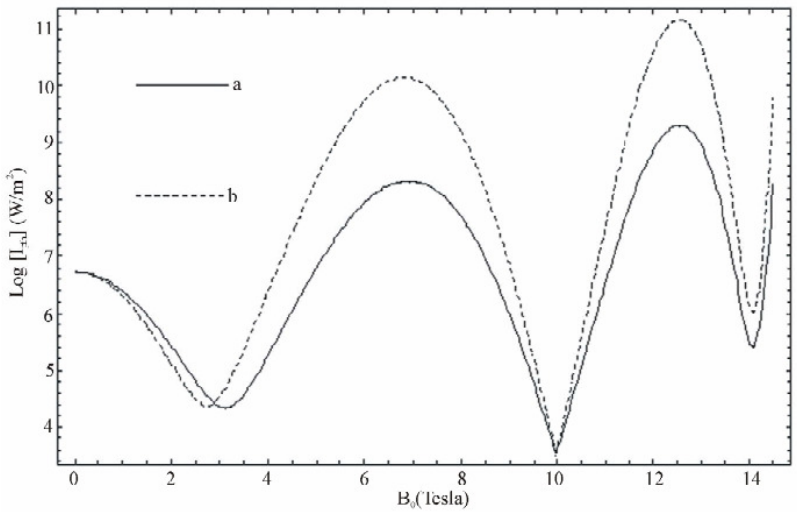

Figure 2: Variation of threshold pump intensity (Log[I_{pth}]), for Equation (12b), with magnetostatic field (B_0) at free carrier concentration (a) $n_0 = 1.5\times10^{19}$ m^{-3} and (b) $n_0 = 2.4\times10^{19}$ m^{-3}.

When $B_0 > 0$, I_{pth} reduces considerably due to resonance conditions. Let us focus on the threshold condition for parametric amplification when piezoelectricity is solely responsible for parametric interaction. In this case, minimum threshold intensity can be achieved in two different range of externally applied magnetostatic field, *i.e.* moderate and strong magnetostatic fields. In former case, a minimum value of threshold intensity is found ~ 1.1×10^3 Wm^{-2} (for $B_0 = 5.0$ T, $n_0 = 2.4\times10^{19}$ m^{-3}). The minima of threshold intensity arises due to resonance condition: $\omega_s^2 = (\omega_c^2 + \gamma^2)/([1-(\Omega_p^2/4\omega_a^2)]$. It is also noticed that the position of minima shifts toward lower magnetostatic field with increasing doping concentration. While in later case, I_{pth} can be achieved when $\omega_p \sim \omega_s \sim \omega_c$. For example, when $B_0 = 14.1$ T, $I_{pth} \sim 1.2\times10^3$ Wm^{-2}. Here it is worth pointing out that in later case a small change in free carrier concentration does not affect shifting position of minima. This result is well in agreement with the result of Palik and Furdyna [25].

In order to study the role of different physical mechanism leading to parametric interaction we have used Equation (12b) to obtain threshold condition for onset of parametric amplification due to coupling between the piezoelectric coefficient and pump electric field. The threshold pump intensity, determined from Equation (12b), versus external magnetostatic field for two different samples having free carrier concentration *i.e.* (a) $n_0 = 1.5\times10^{19}$ m^{-3} and (b) $n_0 = 2.4\times10^{19}$ m^{-3}, is plotted in Figure 2. One may observe that when $B_0 = 0.0$ T, I_{pth} required for onset of parametric amplification is 5.9×10^6 Wm^{-2}. The figure depicts that the minima of I_{pth} is independent of change of free carrier concentration. The model suggests that when $B_0 > 0$, a minimum I_{pth} can be achieved at three different values of magnetostatic field due to three different resonance conditions: $\omega_s^2 = (\Omega_p^2\omega_c^2 + \gamma^2)/\gamma^2$, $\omega_s^2 = 2\omega_c^2 + \gamma^2 + 2\zeta_a\omega_a$, and $\omega_s = \omega_c$. Around the first resonance condition, the minimum I_{pth} is found to be 3.0×10^4 Wm^{-2}. This resonance condition also shifts the position of minima towards lower magnetostatic field with increase in free carrier concentration. However, the second and the third resonance conditions yield $I_{pth} \sim 1.1\times10^3$ Wm^{-2} and 1.9×10^6 Wm^{-2}, respectively. It is noticed that around the second and third resonance conditions the position of minima are nearly independent with the variation of doping concentrations. A comparison of the results obtained from Equation (12a) and (12b) reveal that the required minimum I_{pth} for the onset of parametric amplification due to parametric coupling of piezoelectric coefficient and pump electric field is nearly 100 times higher than the value obtained due to solely piezoelectricity. In the forthcoming analysis to study the behavior of parametric gain we consider $I_p = 1.5\times10^{11}$ Wm^{-2} as a representative excitation intensity which is well above the threshold intensity but below the damage threshold of the sample [26].

The Equation (13) with (12) shows the dependence of parametric gain on controllable physical parameters namely free carrier concentration (through plasma frequency, Ω_p), external applied magnetostatic field (through cyclotron frequency, ω_c) and pump Intensity (I_p).

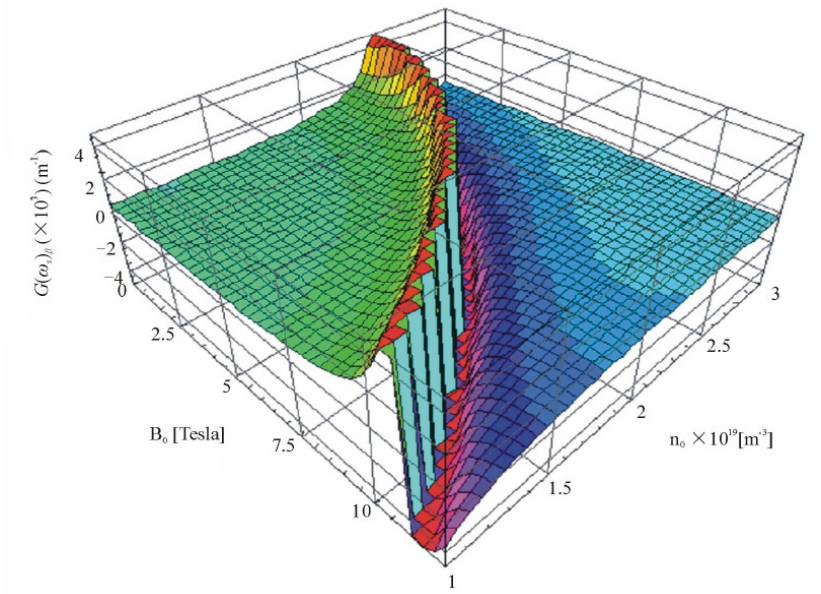

Figure 3: Variation of $(g(\omega_s)_\beta)$ with magnetostatic field (B_0) and free carrier concentration (n_0).

Figure 3 shows the behavior of parametric gain at stokes frequency $(g(\omega_s)_\beta)$, obtained using Equation (13) with Equation (12a), by varying B_0 and n_0 simultaneously. The figure clearly shows substantial enhancement of $g(\omega_s)_\beta$ and change in its sign. This typical behavior arises due to resonance condition:

$$\omega_s^2 = (\omega_c^2 + \gamma^2)/([1-(\Omega_p^2/4\omega_a^2)]$$

(resonance between scattered stokes wave frequency and modified electron-cyclotron wave frequency). At the resonance condition, magnetostatic field dependent drift velocity becomes many times larger than the acoustic wave velocity and due to which interaction between plasmon and acoustic

phonon becomes strong. The resonance condition allows one to select typical value of B_0 and n_0 at which maximum gain can be achieved. A small change in typical value of B_0 and n_0 leads to decrease in the value of positive gain coefficient and further change gives rise to maximum negative gain (*i.e.* maximum absorption).

By selecting appropriate value of B_0 (say 9.0 T) and n_0 (say 1.5×10^{19} m^{-3}), we obtained $g(\omega_s)_\beta$ ~ 396 m^{-1}. By varying B_0 and n_0 simultaneously, the change in sign of $g(\omega_s)_\beta$ can also be observed. Besides, it is noticed that when the sample is subjected to moderate magnetostatic field, *i.e.* $0.0 < B_0 < 10.5$T, the value of $g(\omega_s)_\beta$ varies almost parabolically with rising n_0. The theoretical model also suggests possibilities of shifting in frequency of coherent backward stokes modes towards higher value of B_0 (*i.e.* blue shift) as plasma frequency (through n_0) approaches twice of acoustic wave frequency. After departure from the resonance condition, the parametric gain

becomes negative (absorption) and saturates to very small value. However, in the absence of external magnetostatic field ($B_0 = 0$) and $n_0 = 1.5\times10^{19}$ m^{-3}, the value of $g(\omega_s)_\beta$ is 7.4 m^{-1} which is nearly 50 times smaller than the value obtained around the resonance condition.

The salient feature of result is the switching of positive and negative gain between high value to low value by varying independently/simultaneously B_0 and n_0 and also achieving its large value in $A^{III}B^{V}$ weakly piezoelectric semiconductors. The result suggests the possibility of devise of parametric switches in far infrared region.

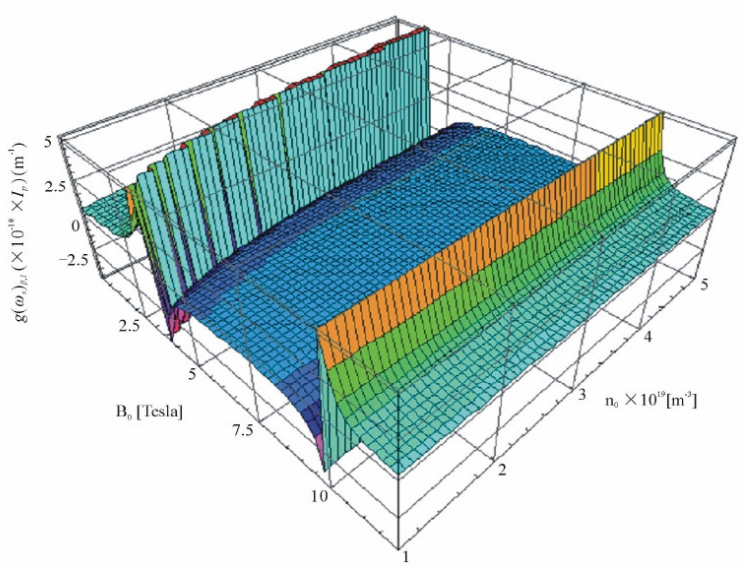

Figure 4: Variation of $g(\omega_s)_{\beta,I}$ with magnetostatic field (B_0) and free carrier concentration (n_0).

Figure 4 shows variation of the gain coefficient $g(\omega_s)_{\beta,I}$, using Equation (12b), with respect to B_0 and n_0. This figure also depicts the enhancement of $g(\omega_s)_{\beta,I}$ as well as change in its sign. In this case, enhancement and switching of the gain occurs due to resonance conditions: $\omega_s^2 = (\Omega_p^2\omega_c^2 + \gamma^2)/\gamma^2$ and $\omega_s^2 = 2\omega_c^2 + \gamma^2 + 2\zeta_a\omega_a$. Interesting feature of this case is the interaction between plasmon oscillator and electron-cyclotron oscillator in the presence of excitation intensity. It is often advantageous, moving the frequency of coherent stokes wave to higher and more accessible spectral region in proportion to: (a) plasma frequency (or n_0) for fixed electron cyclotron frequency (or B_0), (b) electron-cyclotron frequency for fixed plasma frequency, and (c) combination of both frequencies. For example, in moderately doped semconconductor ($n_0 = 1.5\times10^{19}$ m^{-3}), low externally applied magnetostatic field (1.5 - 3.0 T) yields a large value of $g(\omega_s)_{\beta,I}$ and also alters its sign as well as shifts the stokes frequency towards higher frequency (Blue shift). With further increase in B_0, the second resonance condition ($\omega_s^2 = 2\omega_c^2 + \gamma^2 + 2\zeta_a\omega_a$) yields sharp enhancement and change of sign of $g(\omega_s)_{\beta,I}$ at $B_0 = 10.0$ T.

The parametric gain can be improved in addition to the B0 and n0 dependence by raising the excitation intensity value. It is important to note that, practically speaking, the excitation intensity cannot be increased arbitrarily because doing so could cause the sample to lose its optical integrity [26].

4. Conclusions

In the current work, weakly piezoelectric narrow direct-gap $A^{III}B^{V}$ doped semiconductors such n-InSb subjected to a transverse magnetostatic field under an off-resonant transition regime were used to explore the operational characteristic of the parametric amplifier utilising electromagnetic treatment. It is possible to make the following significant conclusions:

1. The effect of doping level, transverse magnetostatic field, and pump intensity on operational characteristics of parametric amplifiers (i.e. threshold condition and optical parametric gain/ absorption) in piezoelectric $A^{III}B^{V}$ doped semiconducting crystals properly illuminated by slightly off-resonant not-too-high-power pulsed lasers with pulse duration sufficiently larger than the acoustic wavelength has been successfully studied using the hydrodynamic model of semiconductor-plasma.
2. Resonance conditions between (i) lattice frequency and plasma frequency, (ii) stokes frequency and electron-

cyclotron frequency, (iii) stokes frequency and hybrid (plasma and electron-cyclotron) frequency may be utilized, on one hand, to reduce the threshold intensity for onset of parametric amplification. On the other hand, switching of parametric gain between the low and high value and hence open up the possibility of devising optical switch. A strong transverse magnetostatic field (10.0 T) enhances the gain by a factor of 10^3 as in its absence.

3. A magnetoactive $A^{III}B^{V}$ semiconductor-plasma's technological promise as a host for parametric devices like parametric amplifiers and oscillators is established. Under resonance conditions, parametric amplification and oscillation in the infrared regime in $A^{III}B^{V}$ crystals replace the traditional idea of employing high power pulsed lasers.

References

[1] R.L. Bayer, Nonlinear Optics, Academic Press, London (1975), pp. 47-159.

[2] C.K. Hong, L. Mandel, Theory of parametric frequency down conversion of light, *Phys. Rev. A* **31** (1985) 2409-2418.

[3] Z.Y. Ou, L.J. Wang, L. Mandel, Photon amplification by parametric sown conversion, *J. Opt. Soc. Am. B* **7** (1990) 211-214.

[4] J. Zyss, I. Leodoun, J. Badan, J. L. Oudar, J. Etchepare, D. Hulin, A. Mingus, A. Antonnetii, Amplification at emission paramétriques à l'Échelle subpicoseconde dans un crystal organique: Application à la Spectroscopy Infra-Rouge, *Revue de Physique Appliquée* **22** (1987) 1229-1238.

[5] D.A.B. Miller, Bistable optical devices: Physics and operating characteristics of nonlinear optics in semiconductors, *Laser Focus* **19** (1983) 61-68.

[6] R.K. Jain, Degenerate four-wave mixing in semiconductors: Application to phase conjugation and to picoseconds resolved studies of transient carrier dynamics, *Optics Engineering Bellingham* **21** (1982) 199-218.

[7] S.D. Smith, Lasers: Nonlinear optics and optical computers, *Nature* **316** (1982) 319-324.

[8] P.A. Wolff, Nonlinear Optics, Academic Press, London (1977), pp. 169-212.

[9] E. Garmire, Resonant optical nonlinearities in semiconductors, *IEEE J. Quant. Electron.* **6** (2000) 1094-1110.

[10] R.W. Boyd, Nonlinear Optics, Academic Press, San Diego (1992), ch. 9, pp. 409-450.

[11] M.J. Connelly, Semiconductor Optical Amplifiers, Springer-Verlag, Boston (2002).

[12] D. Apostolopoulos, K. Vyrsokinos, P. Zakynthinos, N. Pleros, H. Avramopoulos, An SOA-MZI NRZ wavelength conversion scheme with enhanced 2R regeneration characteristics, *IEEE Photon. Tech. Lett.* **21** (2009) 1363-1365.

[13] A. Hayat, Y. Elor, E. Small, M. Orenstein, Phase matching in semiconductor nonlinear optics by linear long-period gratings, *Appl. Phys. Lett.* **92** (2008) 181110-112.

[14] G. Lutz, Semiconductor Radiation Detectors: Device Physics, Springer, Berlin (1999).

[15] Y. Fu, M. Willander, Physics Models of Semiconductor Quantum Devices, Springer, Berlin (1999).

[16] M.B. Johnston, D.M. Whittaker, A. Dowd, A.G. Davies, E.H. Linfield, X. Li, D.A. Ritchie, Generation of high-power terahertz pulses in a prism, *Opt. Lett.* **27** (2002) 1935-1937.

[17] G. Meinert, L. Banyai, P. Gartner, H. Haug, Theory of THz emission from optically excited semiconductors in crossed electric and magnetic fields, *Phys. Rev. B* **62** (2000) 5003-5009.

[18] J.M. Makowska, K.J. Plucinski, A. Hruban, J. Ebothe, J.I. Fuks, I.V. Kityk, Acoustically induced optical second harmonic generation in InAs, *Semicond. Sci. Technol.* **19** (2004) 1285-1290.

[19] A.A. Bulgakov, O.V. Sharmkova, Nonlinear interaction of waves in semiconductor plasma, *J. Phys. D*: *Appl. Phys.* **40** (2007) 5896-5901.

[20] B. Lal, P. Aghamkar, S. Kumar, M.K. Kashyap, Second-order optical susceptibility in doped III-V piezoelectric semiconductors in the presence of a magnetostatic field, *Eur. Phys. J. D* **61** (2011) 717-724.

[21] P.K. Kaw, Parametric excitation of ultrasonic waves in piezoelectric semiconductors, *J. Appl. Phys.* **44** (1973) 1497-1498.

[22] D.L. Spears, Brillouin scattering study of propagating acoustoelectric domains in *n*-GaAs, *Phys. Rev. B* **2** (1970) 1931-1951.

[23] D.L. Rode, Semiconductors and Semimetals, Academic, New York (1975), ch. 1, pp. 5-17.

[24] G.E. Stillman, C.M. Wolfe, J.O. Dimmock, Hall coefficient factor for polar mode scattering in *n*-type GaAs, *J. Phys. Chem. Solids* **31** (1970) 1199-1204.

[25] E.D. Palik, J.K. Furdyna, Infrared and microwave magnetoplasma effects in semiconductors, *Rep. Prog. Phys.* **33** (1970) 1193-1322.

[26] J.M. Mayer, F.J. Bartoli, M.R. Kruer, Optical heating in semiconductors, *Phys. Rev. B* **21** (1980) 1559-1568.